5-2014

Cryoprotectant Loading in a Microchannel

Shelby Pursley

Cryoprotectant Loading in a Microchannel

by

Shelby Pursley

Undergraduate honors thesis under the direction of

Dr. W. Todd Monroe

Department of Biological and Agricultural Engineering

Submitted to the LSU Honors College in partial fulfillment of

the Upper Division Honors Program.

May 2014

Louisiana State University

& Agricultural and Mechanical College

Baton Rouge, Louisiana

CRYOPROTECTANT LOADING IN A MICROCHANNEL

AN HONORS THESIS PROJECT

Shelby Pursley, LSU Biological Engineering

ACKNOWLEDGEMENTS

I would like to acknowledge the faculty and student mentors at Louisiana State University who have aided in the completion of this project as well as my professional development as a researcher and scholar. Thank you to Dr. W. Todd Monroe (LSU Biological and Agricultural Engineering) for his support of this project, his constant presence as a mentor, and for his faith in my abilities. His guidance in my both my research efforts and my professional development have been invaluable to me. Additionally, his respect and understanding for my involvement at LSU outside of the classroom and the lab has enabled my greatest successes. Thank you to Dr. Krishnaswamy Nandakumar (LSU Chemical Engineering) for his support of my research efforts over the last four years. His promotion of my abilities and faith in my intellect over the years has been instrumental in my development. Thank you to Dr. Tom Scherr for his guidance, trust, and patience in the last four years. It was because of his willingness to invest time and energy in my development that I have enjoyed success in the world of academia. I have been lucky to have him as a mentor and a friend.

Collaborations are an exercise in compromise and compassion. I am grateful to have enjoyed many collaborators through this project. Thank you to Amy Guitreaux without whom none of my work would have been possible. Her patience, collaborative spirit, and company have been the perfect pairing to her expertise and model work ethic. Thank you to Dr. Terrence Tiersch (LSU Aquaculture Research Station, ARS) for the use of the facilities at ARS and his support of countless microfluidic engineering projects. Thank you to Jacob Beckham (LSU Biological Engineering) for his assistance in all things microfabrication and to Dr. Adam Melvin (LSU Chemical Engineering) for the use of his fabrication facilities.

Lastly, thank you to my friends and family who have withstood my constant state of frenzy in the last four years as I strove to be the girl that does it all and does it all well. You have done so with the patience and compassion that garners sainthood, and I am grateful.

TABLE OF CONTENTS

ABSTRACT

Contemporary biological, agricultural, and medical research is dependent on the successful cryopreservation of cells for off the shelf availability of biological samples and the cataloging of cell lines. At Louisiana State University (LSU), the Aquaculture Research Station (ARS) leads research efforts related to cryopreservation of germplasm of aquatic species and has partnered with the LSU Biological Engineering Department to seek new small volume, high throughput approaches to existing cryopreservation protocols through the use of microfluidic devices. In this first step by our group into cryopreservation on chip, the focus of this project was to develop microfluidic approaches to exposing biological cell samples to cryoprotective agents (CPA's, cryoprotectants) to dehydrate cells in preparation for freezing. A straight T-channel 12.5 cm in length was proposed as an ideal environment for CPA loading. First, the proposed device design and potential operating parameters were simulated through rigorous mathematical modeling. Next, devices were fabricated using standard photolithography processes established in literature. Though there is a vested interest in developing technologies and protocols specific to the cryopreservation of zebrafish (*Danio rerio*) sperm, sperm samples from koi carp (*Cyprinus carpio*) were used for testing of device prototypes. From these efforts in modeling and device development, we illustrate the phenomena associated with cryoprotectant loading in a microchannel, demonstrate cell toxicity outcomes for cryoprotectant loading in a microfluidic device, and make recommendations on the future implementation of this technology in the laboratory.

CHAPTER 1. FOREWORD

This document seeks to present a cohesive look at the efforts in microfluidic cryoprotectant loading of sperm cells made under the guidance of Dr. W. Todd Monroe. Before explaining the motivation of this work, one should understand the motivation to pursue microfluidic approaches to the handling of germplasm and the specific collaboration between the labs of Dr. Monroe and Dr. Terrence Tiersch (LSU ARS).

The LSU Aquaculture Research Station has vested interest in research to aid the local aquatic farming industry and is the clear leader for cryopreservation research in the region. ARS is also interested in cryopreservation research related to zebrafish (*Danio rerio*) germplasm, as zebrafish are a commonly used model in many areas of biomedical research [10,16,45,32]. One of the main hurdles in developing germplasm handling protocols for any species is ensuring standardization and reproducibly. For the handling of zebrafish samples, there is the additional challenge of developing protocols for small volumes (< 1 mL), which can keep samples from different genetic strains or even individual fish separate in cryopreserved catalogs [48]. Thus, a partnership was forged between Dr. Tiersch's aquaculture group and Dr. Monroe's bio-MEMS (biological microelectromechanical systems) group to seek small volume, high throughput devices for germplasm handling that would enable further standardization in the field and enable biomedical research.

There have been efforts to introduce a microfluidic approach at almost every step in the gamete handling process within these groups [38,43,48,52], but the work presented here showcases the first efforts in applying this approach to the cryoprotectant loading process. Through an additional collaboration with the LSU Chemical Engineering Department, we take an interdisciplinary approach to confront this challenge mathematically and experimentally.

CHAPTER 2. INTRODUCTION

The cryopreservation of cells and tissues is instrumental for a variety of disciplines and industries as it provides critical to long-term storage and off-the-shelf availability of biological samples [9,27,28,31,34,47,53]. Typical cryopreservation protocols aim to remove intracellular water to avoid damaging intracellular ice formation (IIF) by exposing the sample to a cryoprotective agent (CPA), thus creating an osmotic pressure gradient [20]. Cryoprotectants can be either permeable, which replace the water inside the cell, or impermeable, which simply dehydrate the cell [7,20]. While CPAs are useful in preventing cell damage due to IIF, the dehydration process can induce harmful osmotic shock [7,9,45], and the CPAs themselves have significant cytotoxic effects [2,7,20]. In the use of CPAs for cryopreservation, there is a tradeoff between the necessary prevention of IIF and the detrimental effects of the associated osmotic shock and cytotoxicity. Both experimental studies and numerical modeling efforts seek to develop effective protocols for the loading of CPAs into biological samples to improve viability by optimizing this trade-off [8,12,13,35,39,51].

Experimentally, the balance in this trade-off has been sought by utilizing two or more cryoprotectants in sample treatment (a "cryoprotectant cocktail"). When using a cocktail system, the tandem use of a permeating and non-permeating CPA has been shown to require lower concentrations of both species than would be required if each worked alone to achieve the desired effect [27,33]. The risk of adverse cytotoxic effects for a given species can thus be reduced in a cocktail system by decreasing the concentration of a CPA. Though a CPA cocktail can provide advantages over a singular CPA system, there are still further benefits to be gained by optimizing the cocktail system. The chemical species present in a cocktail, the concentrations of the chemicals present, the exposure time of a biological sample to a cocktail or cryoprotectant, and the order in which these chemicals are introduced to the sample are all operating parameters that provide control in the removal of intracellular water while minimizing osmotic shock.

Microfluidics have previously shown promise in minimizing osmotic shock during cryoprotectant loading [45], and there has been a resulting surge in studies of single CPAs in microchannels [14,15, 22,36]. The stable, laminar flow at low Reynolds ($Re = \frac{\rho U L}{\mu}$) numbers allows for gradual introduction of cells to cryoprotectants, thus keeping the water flux and cryoprotectant flux below lethal levels which can result in greater cell survival rates during loading and subsequent cryopreservation [45].

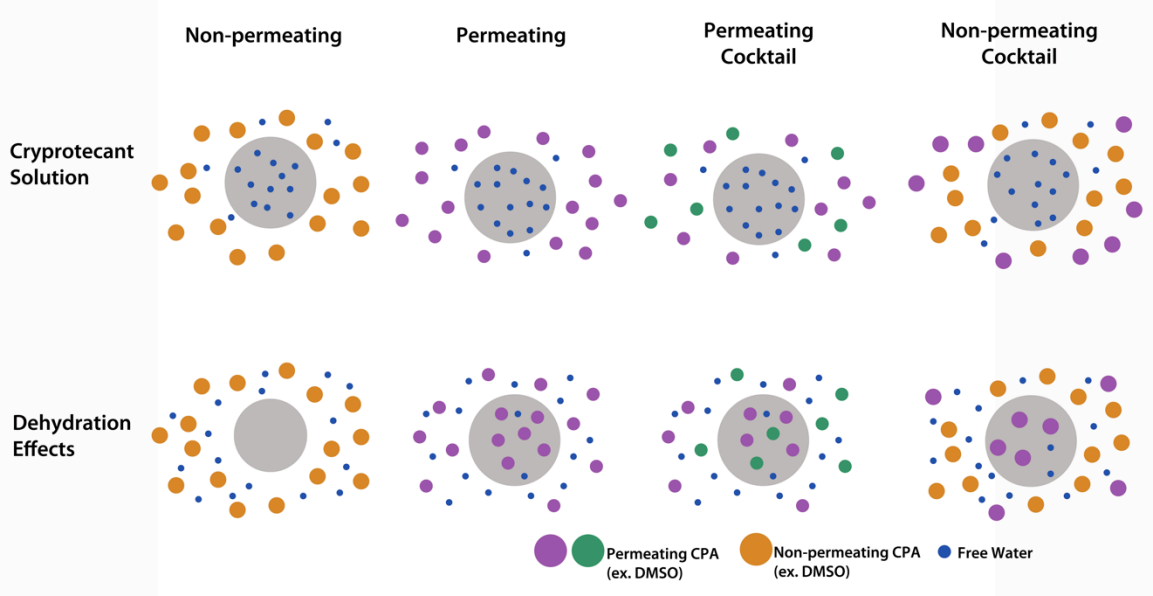

FIGURE 1: CRYOPROTECTANT TREATMENTS. Here we give a simplistic visualization of cryoprotectant treatment strategies for dehydration. The top row shows a representative cell in a cryoprotectant solution, and the bottom row shows the expected dehydration effects due to the osmolality gradient across the cell membrane as well as the cryoprotectant loading that may occur when permeable CPA's are used. This does not represent in any way the relative efficacies of any treatment in removing free water from the intracellular space, but illustrates the expected experience of the cell for a given CPA treatment type.

As stated previously, the cocktail system approach, though an improvement upon a single cryoprotectant treatment, leaves much room for further improvement by fine-tuning the relevant parameters. Introducing a microfluidic protocol in this process would enable fine tuned control of these parameters in the CPA loading process and provide predictable and reproducible exposure of biological samples to cryoprotectants in a given cocktail. The complex nature of a CPA cocktail loading system coupled with the variations in a population of cells in a microchannel render experimental efforts to optimize microfluidic CPA loading protocols highly inefficient. A realistic model for a cocktail treatment in a microchannel is necessary for understanding the loading of CPA at a molecular level and improving cryopreservation protocols.

Many groups in the cryopreservation field have employed microfluidic approaches for empirical determinations of membrane transport parameters and the monitoring of single cells (often eggs) under the influence of cryoprotectants [4,5,23,49], but at this point none have harnessed the flow characteristics within a microchannel for optimized cryoprotectant loading. Others in the field have made a similar argument on the advantages of a microfluidic approach to cryoprotectant loading and

sought to model these hypothesized phenomena [45], but each of these efforts neglected to account the distribution of intracellular CPA concentration across a population of cells due to the parabolic velocity profile in a microchannel or investigate the more industry relevant use of a cryoprotectant cocktail.

In this work, we propose a straight T-channel 12.5 cm in length as an ideal environment for CPA loading. First, proposed device designs and potential operating parameters for both single CPA systems and CPA cocktail systems were simulated through rigorous mathematical modeling that takes into account the population distributions resulting from flow in a microchannel. Next, devices were fabricated using standard photolithography processes to investigate the capacity of the proposed microfluidic device to temper osmotic shock and cytotoxic effects of a CPA treatment. From these efforts in modeling and device development, we illustrate the phenomena associated with cryoprotectant loading in a microchannel, demonstrate cell toxicity outcomes for cryoprotectant loading in a microfluidic device, and make recommendations for future implementation of this technology in the laboratories.

CHAPTER 3. MODELING CRYOPROTECTANT LOADING IN A MICROCHANNEL

Mathematical modeling uses first principles to simulate an event in nature. In the field of microfluidics, modeling is an especially useful tool for understanding phenomena at the micro-scale and quantifying variables difficult or seemingly impossible to measure with current instrumentation. In this chapter, the methods for modeling cryoprotectant loading in a microchannel are outlined to show the correlation between input parameters and outcomes. Additionally, several results of interest are highlighted to demonstrate principles that will govern CPA loading in a microchannel in a laboratory. Input modeling parameters, full simulation results and model validation have been omitted, but can easily by found by consulting published findings on this work [40,41,42].

To investigate the capacity for cryoprotectant loading in a microchannel, we simulate the loading of several single cryoprotectants and a common cryoprotectant cocktail into cells within a microchannel. For the single cryoprotectant system, we develop a modeling framework for cryoprotectant loading in a microchannel that accounts for distributions in cell outcomes based on Poiseuille flow in a microchannel [44] and look at correlations between CPA loading and flowrates for human embryonic kidney (HEK) cells, a cell line with well known CPA membrane transport parameters. In this loading system, a straight 12.5 cm T-channel is used as an ideal environment for diffusion based mixing. In the cocktail system, we investigate the common cocktail DP6, consisting of 1,2–propanediol (propanediol, PD) and DMSO. While DP6 typically contains HEPES, an organic buffer commonly used in cell culture, our study examines only PD and DMSO as they are commonly used together in conjunction with any number of chemical species [11]. In this loading system there is a pair of upstream inlets for one CPA that are perpendicular to the central sample inlet, and a second set of sheath inlets 12.5 cm downstream for the second CPA. The loading system investigates the microfluidic equivalent to a multi-step batch process, but could ultimately provide maximum control of cytotoxic factors. Of particular interest in the cocktail case is the interacting of miscible fluids of varying viscosities in a microchannel. Special emphasis is given to understanding the unique flow patterns that occur in a microchannel in this proposed cocktail case.

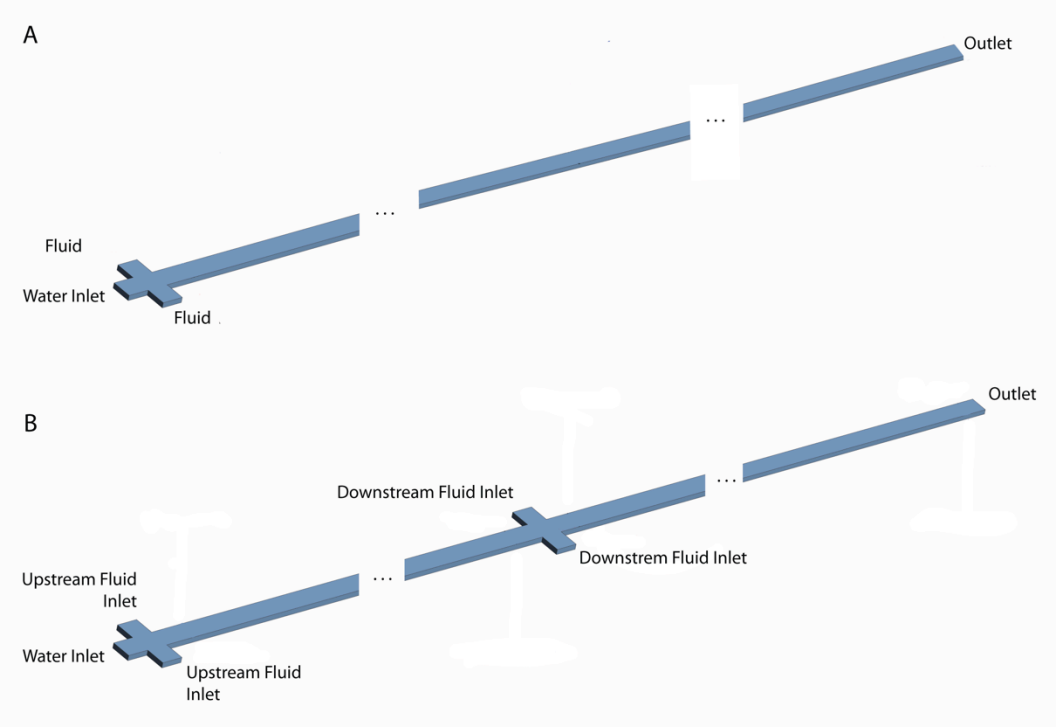

FIGURE 2: SCHEMATIC OF MICROCHANEL GEOMETERIES. Renderings of microchannel domains constructed for numerical simulations of (A) single cryoprotectant cases and (B) cryoprotectant cocktail cases. Both geometries are identical with the exception that the cocktail geometry has a second set of inlets exactly half way down the length of the channel. The channels are 200 µm in width, 50 µm in depth, and 12.5 cm in length from the fluid junction at the main inlet.

3.1 METHODS

Fluid Flow Modeling

The fluid dynamics package FLUENT v13.0 (ANSYS Inc., Canonsburg, PA) was used to solve the steady- state conservation of mass (eq (1)), conservation of momentum (eqs (2 – 3)), and species continuity equations (eqs (4 – 5)).

$$\nabla \cdot (\rho u) = 0 \tag{1}$$

$$\nabla \cdot (\rho u u) = -\nabla P + \nabla \cdot (\tau) + \rho g \tag{2}$$

$$\tau = \mu \left[\left(\nabla u + \nabla u^T \right) - \frac{2}{3} \left(\nabla \cdot u I \right) \right] \tag{3}$$

$$\nabla \cdot (\rho u X_i) = -\nabla \cdot J_i \tag{4}$$

$$J_i = -\sum_{j=1}^{N-1} \rho D_{ij} \nabla X_j \tag{5}$$

In eqs (1-5): u is the fluid velocity, P is the fluid pressure, ρ is the local density of the mixture, μ is the local viscosity of the mixture, D_{ij} is the binary diffusivity of component i in component j, and X_j is the mass fraction of component j. Boundary conditions for the simulations were as follows: no-slip velocity at the channel walls; a zero-pressure outlet; constant normal inlet velocity (varied for each flow rate); and constant concentration of the cryoprotectant introduced at the cell inlet junction.

For the cryoprotectant cocktail case, diffusivity and viscosity were not assumed constant due to the large disparity in the fluid properties (e.g. viscosity) of each cryoprotectant. In a given local environment (volume element), the mass fraction of each cryoprotectant present largely affects the effective fluid properties of the locale.

Particle Tracking

Lagrangian particle tracking was used in FLUENT (ANSYS, Inc.) to simulate cells as inert spherical particles inside the channel. Once the steady state flow field is solved, spherical particles are released from each finite volume element face on the center inlet. The position and velocity of the particles as they progress through the micro-device are calculated by solving the force balance on the particles,

$$\frac{du_p}{dt} = F_D\left(u_f - u_p\right) + g\frac{\left(\rho_p - \rho_f\right)}{\rho_p} + F \qquad (6)$$

$$F_D = \frac{18\mu}{\rho_p d_p^2}\frac{C_D Re_p}{24} \qquad (7)$$

$$Re_p = \frac{\rho_f d_p \left|u_p - u_f\right|}{\mu} \qquad (8)$$

$$F = \frac{2K\nu^{\frac{1}{2}}\rho_f d_{ij}}{\rho_p d_p \left(d_{lk}d_{kl}\right)^{\frac{1}{4}}}\left(u_{j,f} - u_{j,p}\right) \qquad (9)$$

In eqns (6) – (9), F_D is the drag force on the particle, u_f is the fluid velocity, u_p is the particle velocity, g is the acceleration due to gravity, q_p is the particle density, q_f is the fluid density, F is the Saffman lift force due to shear, C_D is the drag coefficient for smooth and spherical particles, Re_p is the particle Reynolds number, d_p is the particle diameter, K is a constant coefficient of Saffman's lift force (and is set to 2.594), v is the fluid kinematic viscosity, and d_{ij} is the deformation tensor.

Though particles are assigned a diameter and a density to solve the force balance on each particle, the model treats particles travelling through the channel as point particles and therefore does not take into account particle-particle interactions in the channel. Additionally, because these particles are

treated as points in space, the fluid flow field does not reflect any changes as a result of the resultant volume of the cells occupying any given space in the channel.

These equations were solved every time step (0.001 s) for each particle throughout the length of the channel. For each time interval, the position vector, velocity vector and local external CPA concentration for each particle are giving a detailed individual history for all particles.

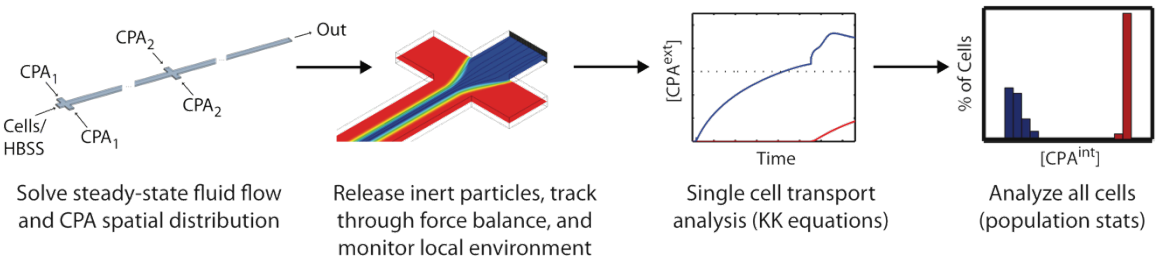

FIGURE 3: MATHEMATICAL MODELING SCHEMATIC. Flow diagram showing the order of operations for mathematical modeling of cryoprotectant loading in a microfluidic channel and the source of intracellular CPA concentration data for a population of cells.

Membrane Transport Modeling

Extracellular concentration data is then used in the Kadem-Katchalsky (KK) equations for coupled solvent-solute transport across a cell membrane [17,29,30] in MATLAB. Depending on the cryoprotectant scheme, some or all of the following associated definitions for the KK equations are required (eqns (13) – (16)):

$$J_w = \frac{1}{A_c}\frac{dV_w(t)}{dt} = -L_p RT\left\{\Delta C_{salt} + \sigma_{DMSO}\Delta C_{DMSO} + \sigma_{PD}\Delta C_{PD}\right\}, \tag{10}$$

$$J_{DMSO} = \frac{1}{A_c}\frac{dN_{DMSO}(t)}{dt} = \bar{C}_{DMSO}(1-\sigma_{DMSO})J_w + P_{DMSO}\Delta C_{DMSO}(t), \tag{11}$$

$$J_{PD} = \frac{1}{A_c}\frac{dN_{PD}(t)}{dt} = \bar{C}_{PD}(1-\sigma_{PD})J_w + P_{PD}\Delta C_{PD}(t). \tag{12}$$

$$\Delta C = C^{out} - C^{in} \tag{13}$$

$$C^i_{salt}(t) = C^i_{salt}(0) \times \left(\frac{V(0) V_b - \sum \bar{V}_{CPA} N^i_{CPA}(0)}{V(t) V_b - \sum \bar{V}_{CPA} N^i_{CPA}(t)} \right) \tag{14}$$

$$C^i_{CPA,k}(t) = \left(\frac{N_{CPA,k}(t)}{V(t) V_b - \sum \bar{V}_{CPA} N^i_{CPA}(t)} \right) \tag{15}$$

$$\bar{C}_{CPA} = \frac{C^e_{CPA} - C^i_{CPA}}{\ln \frac{C^e_{CPA}}{C^i_{CPA}}} \tag{16}$$

In eqs. (10-16): J_w is the water flux, J_{DMSO} is the DMSO flux , for the cocktail case J_{PD} is the PD flux, N_{DMSO} is the intracellular moles of DMSO, N_{PD} is the intracellular moles of PD, A_c is the surface area of the cell, V_w is the water volume inside the cell, L_p is the hydraulic conductivity of the cell membrane, R is the universal gas constant, T is the temperature, P_i is the permeability of species i, σ_i is the reflection coefficient of species i, $C^i_{salt}(0)$ is the initial intracellular salt concentration, $V(0)$ is initial cell volume, V_b is the osmotically inactive volume of the cell, V_{CPA} is the partial molar volume of the CPA, $N^i_{CPA}(0)$ is the initial intracellular moles of CPA, $V(t)$ is the total cell volume, $N^i_{CPA}(t)$ is the intracellular moles of CPA at time t, and the summations are over the appropriate cryoprotectant chemical species for each case.

In the single cryoprotectant scheme only eqns (10) – (11) are needed, where DMSO can be substituted for any single cryoprotectant for which the membrane transports parameters are known and the concentration of the second species (C_{PD}) would be zero. For the cryoprotectant cocktail scenario, eqns (10) – (12) must be employed to account for the effects of both DMSO and PD.

3.2 Results

Single Cryoprotectant System

Of particular interest in the single cryoprotectant system is the correlation between CPA loading and flowrate and the large distributions in population outcomes for CPA loading due to Poiseuille flow that has been previously ignored in literature.

Firstly, we find the correlation between flowrate and CPA loading in a microchannel is an inverse relationship. For any representative particle in a microchannel we see the extracellular concentration of CPA in the channel quickly reach an equilibrium value due to short diffusion path length in a microchannel while the intracellular concentration of CPA lags behind due to slow transport across the cellular membrane. At the lowest flowrates, we see complete loading of CPA prior to the cell exiting the channel. At higher flowrates we see little or negligible CPA loading as the cell exits the channel.

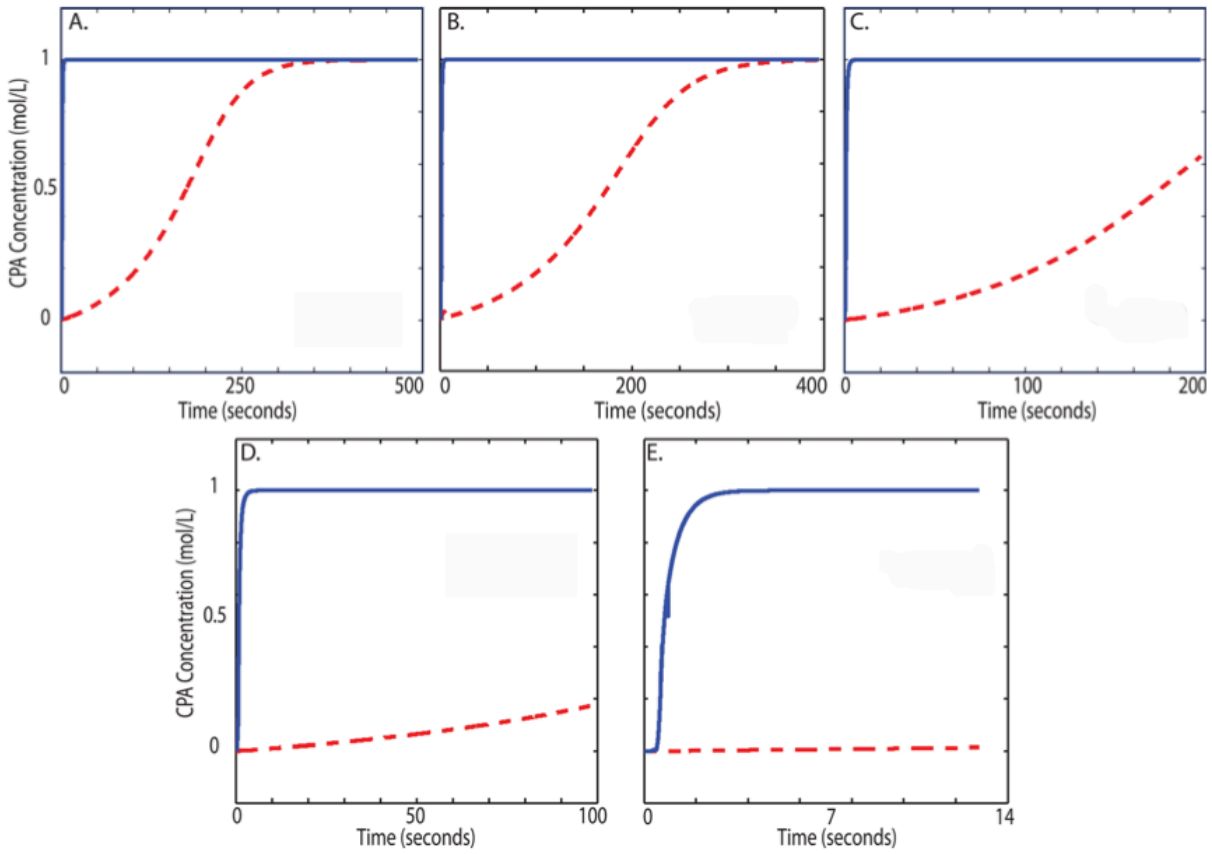

FIGURE 4: TRANSIENT CONCENTRATION AS A FUNCTION OF FLOWRATE. For one of the representative particles released from the inlet, the solid line shows the extracellular CPA concentration and the dashed line shows the intracellular CPA concentration over time for the entire residence time of the particle at the following flowrates: (A) 0.08 μL/min, (B) 0.1 μL/min, (C) 0.2 μL/min, (D) 0.4 μL/min, and (E) 3 μL/min. As flowrate increases, the loading of CPA into the cell moves away from equilibrium or complete loading, defined as intracellular CPA concentration matching extracellular CPA concentration at the outlet.

Also of interest would be the variation in cellular histories and outcomes throughout the channel as result of parabolic flow profiles in a microchannel. Here we see a negative correlation between flowrate residence time distributions. At low flowrates, we see widely varying residence times,

and at high flow rates we see very tight distributions were the entire population of cells experience nearly the same residence time. For CPA loading, we see the largest distribution at moderate flow rates. For low flowrates, the residence time is so large that cells that despite the differences in residence times, all cells are able to reach or near complete loading. At high flowrates, the residence times are nearly uniform and similarly uniform loading would be expected. Additionally, the residence times are small enough that little cryoprotectant is able to permeate the cell membrane before the cell exits the channel resulting in even tighter distributions of CPA loading.

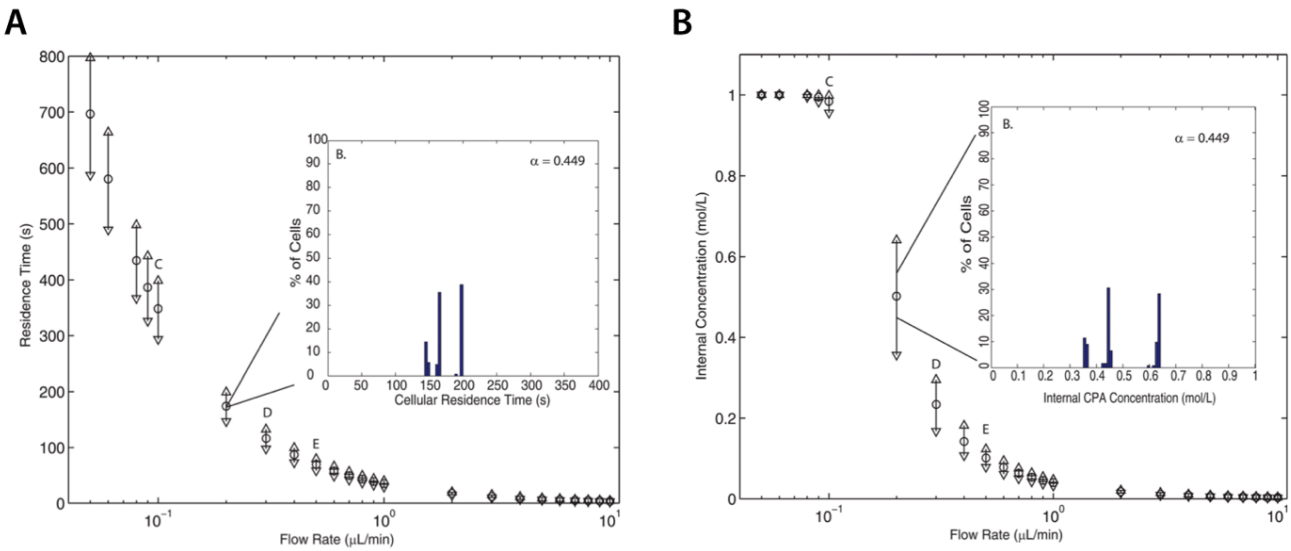

FIGURE 5: DISTRIBUTIONS IN RESIDENCE TIME AND CPA LOADING IN A MICROCHANNEL. Plots show the average (A) residence time and (B) internal CPA concentration at the outlet for a population of particles as a function of flowrate. Error bars show the distribution of values (residence time and internal CPA concentration) for the population and the inset histogram shows the population data for a single flowrate.

Cryoprotectant Cocktail System

Cryoprotectants have widely varying properties, such as density, diffusivity, and molecular weight. Of greatest interest in the proposed cocktail-on-a-chip system is how these viscous and miscible fluids will interact in a microchannel. We model the interactions of DMSO and PD in a microchannel to see the flow patterns that exist and how these might affect the trends seen in a single cryoprotectant case.

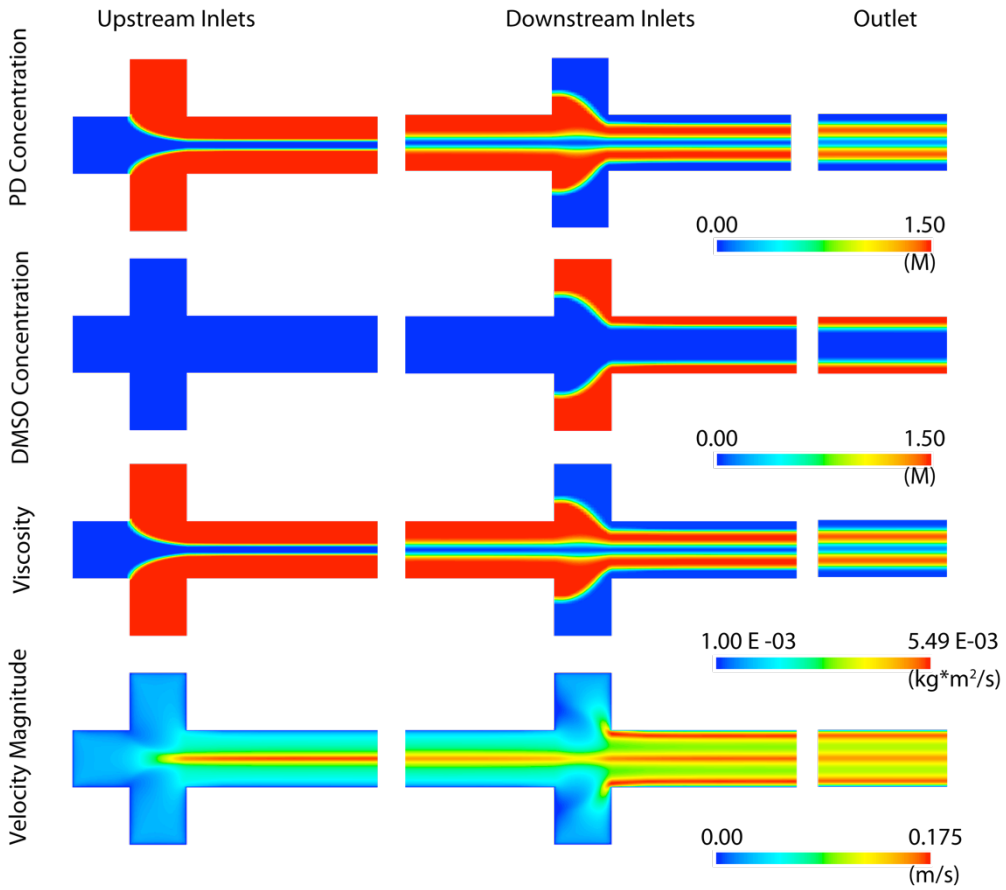

FIGURE 6: CRYOPROTECTANT COCKTAIL IN A MICROCHANNEL – UPSTREAM PD. Color map of variables of interest at steady state in a microchannel where propanediol is introduced at the upstream inlets and DMSO is introduced at the downstream inlets with all inlets at 10 μL/min.

Propanediol is the more viscous fluid and we see in this case from the plots of CPA concentrations that the downstream DMSO inlets do not easily focus the propanediol. In fact, the propanediol seems to push into the DMSO inlet channels and pin the DMSO against the wall of the channel. From the viscosity plot we see viscous threads on either side of the channel centerline. These viscous threads correspond to local minima in fluid velocity, which are atypical of flow in a microchannel and would effect population residence time data shown previously.

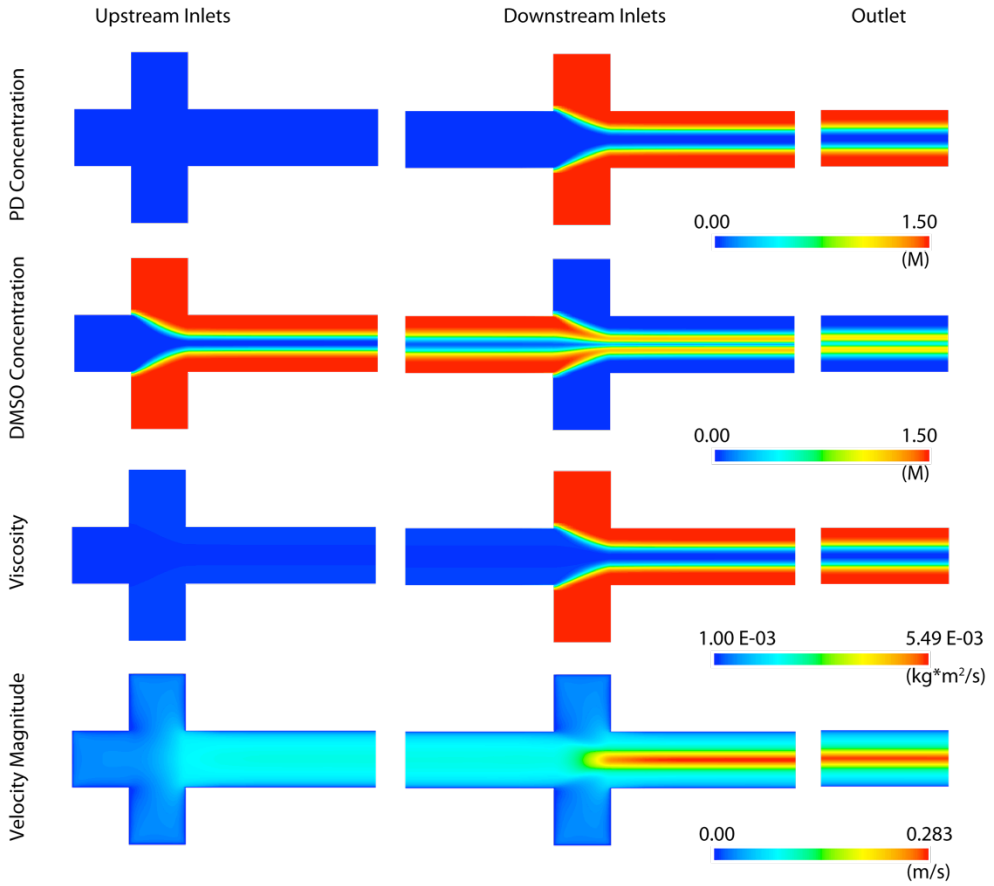

FIGURE 7: CRYOPROTECTANT COCKTAIL IN A MICROCHANNEL – UPSTREAM DMSO. Color map of variables of interest at steady state in a microchannel where propanediol is introduced at the upstream inlets and DMSO is introduced at the downstream inlets.

In the case where the less viscous DMSO is introduced first, we see the channel fluid streams become focused at the downstream inlets by the introduction of propanediol downstream. The propanediol at the wall produces regions of large viscosity that result in more typical velocity profiles across the channel width, but not exactly the parabolic profile usually expected as we see regions of low velocity further from the wall as a result of high viscosity.

3.3 Discussion & Conclusions

We see from the correlation between flowrate and CPA loading that there is great opportunity for optimization for a given protocol in choosing an operating flowrate. For a given cell type and CPA, there will be an ideal flowrate that will allow for gradual CPA loading into the cell and for complete loading to occur at the exact time the cell exits the channel for freezing. This will allow appropriate

intracellular loading of CPA for freezing while exposing the cell to the lowest concentration of CPA for a minimum exposure time. This could have great impact in the use of some highly toxic cryoprotectants that are considered “great cryoprotectants” in the field, but for which a successful protocol to temper toxicity effects does not currently exist.

In the case of cryoprotectant cocktails in a microchannel we see interesting fluid flow patterns that could complicate the optimization of a microfluidic CPA exposure protocol but could also allow for creative strategies to balancing the trade-offs between the inherent osmotic shock and toxicity and the necessary cell dehydration.

These models, though robust, are highly limited due to the need for experimentally derived membrane transport parameters, which vary widely for each combination of a cell type and a CPA species. Additionally, future work in this area should focus equally on CPA loading and free water efflux to better understand the trade-offs that exist between the two. Where these models are more widely impactful is in their ability to shed light on the effects of operating parameters on CPA loading and allow experimentalists to better understand the interworking of such as a system as they pursue ideal laboratory protocols for cryoprotectant loading in a microfluidic device.

CHAPTER 4. ON-CHIP CRYOPROTECTANT LOADING IN THE LABORATORY

With the advanced capabilities of modern microfluidics in thermal cycling and various cell viability assays, it follows naturally that we should seek the implementation of microfluidic technologies to the cryopreservation field. Microfluidics has been used in the field of cryopreservation largely as a tool for monitoring stationary, single cell responses to CPA exposure and experimental determination of membrane transport parameters [4,5,23,49], but at this point the use of microfluidics in cryoprotectant loading protocols has been largely ignored experimentally [6]. The potential advantages of microfluidic protocols for cryopreservation in the laboratory are two-fold: (1) there is a potential advantage for improved cell outcomes discussed previously and (2) many industries and fields that rely on cryopreservation can stand to benefit from the capacity for microfluidics to bring high-throughput, reproducible practices [46,50].

From our models we deduce that a microchannel would be an ideal environment for the introduction of CPA's to cell samples, but are only able to speculate on the potential outcomes of cell fates as a result of tempered osmotic shock or cytotoxicity. Additionally, our modeling efforts take a general approach aimed at understanding the phenomena at play for a wide range of scenarios with no special emphasis on which scenarios are practical for laboratory implementation.

This study seeks to explore the capacity of a traditionally fabricated microfluidic device to load cryoprotectants into cells for cryopreservation in terms of outcomes and feasibility. Our group is interested in the cryopreservation of zebrafish sperm cells, but here we use koi sperm samples for prototyping because koi samples are readily available and the koi sperm cells are extremely similar to zebrafish sperm cells in terms of membrane transport properties and cell size. In this first experimental study, we use N,N-dimethylacetamide (DMA), a permeating and cytotoxic cryoprotectant with a low molecular weight commonly used for the cryopreservation of germplasm in a variety of species [1,3, 20,25,37] as an ideal CPA to compare toxicity outcomes due to cryoprotectant loading at the lab bench-top scale and on-chip.

4.1 METHODS

Device Fabrication

Device fabrication was achieved using traditional photolithography techniques to produce a master mold for polydimethylsiloxane (PDMS) casting. Channel geometries (shown right) were drafted using AutoCAD® (Autodesk, Inc.) and submitted to Front Range PhotoMask (Palmer Lake, CO) for fabrication of a chromium mask. SU-8 photoresist was spun onto a silicon wafer using a spin coater operated under SU-8 manufacturer specified settings to produce a master mold with a uniform structure height of 50 μm. The developed wafer was used to cast PDMS and the PDMS was plasma oxidized to bond to glass for chip fabrication. Inlet leads comprised of syringe tip needles and Tygon tubing (ID = 0.03 in) were inserted at each channel inlet and sealed with PDMS. For the cryoprotectant cocktail design, operational chips were not successfully fabricated.

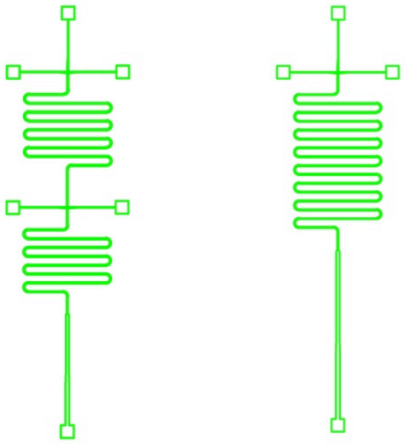

FIGURE 8: CHANNEL GEOMETRIES F FABRICATION. Straight T-Chan geometries modified to fit stand microscope slide blueprint.

Sample Collection

Sperm samples were collected from anesthetized koi carp by squeezing and collected into 2 – 5 mL of HBSS. Sperm sample concentration was determined visually using a Mackler (Sefi-Medical Instruments, Ltd.). Initial sperm sample motility measurements were performed by mixing 20 μL of deionized water with 3 – 5 μL of sperm sample and immediately interrogating with CASA.

FIGURE 9: KOI FISH.

Bench-top Cryoprotectant Loading

In a small test tube, equal parts sperm sample and 18% or 10% DMA solutions were combined to give a resultant treatment of 9% and 5% DMA in HBSS, respectively. Every 5 minutes, the motility of

the sample was assessed using CASA as described previously to give progressive toxicity for the loading of DMA into the sperm cells.

On-Chip Cryoprotectant Loading

Prior to sample processing, the device was pre-filled with HBSS through all inlets at 10 μL/min to remove any air bubbles or debris in microchannels. Next, a syringe containing a portion of the cell sample was driven down the center channel and two syringes, each containing 13.5% DMA in HBSS, were driven through the sheath inlets. All inlets were pressurized equally to produce a uniform, constant flowrate using a multi-channel syringe pump (Harvard Apparatus). The system was allowed to reach steady state (~30 minutes) before samples were collected for interrogation. At the outlet, the outflowing sample was allowed to pool into a small droplet (2 – 3 μL) for collection by pipette and interrogation with CASA. Droplets were tested intermittently after reaching steady state to produce data representative of the entire sample population.

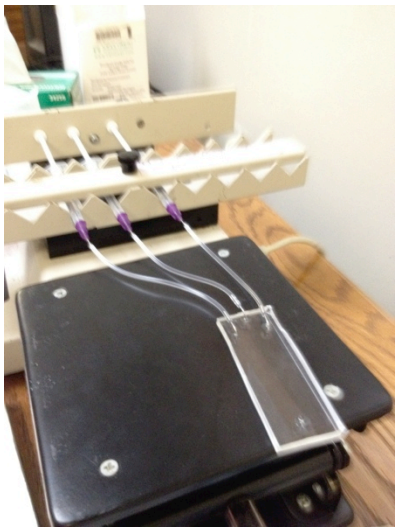

FIGURE 10: EXPERIMENTAL SET-UP FOR SINGLE CPA LOADING IN A MICROFLUIDIC DEVICE.

4.2 RESULTS

Bench-top Cryoprotectant Loading

The concentrations of DMA were chosen based on previous work by the LSU aquaculture group in the cryopreservation of koi sperm cells [19]. We see that 5% DMA is virtually non-toxic at equilibrium. Increasing that concentration to 9%, a concentration more likely needed for successful freezing based on current cryopreservation protocols, is highly toxic to cells.

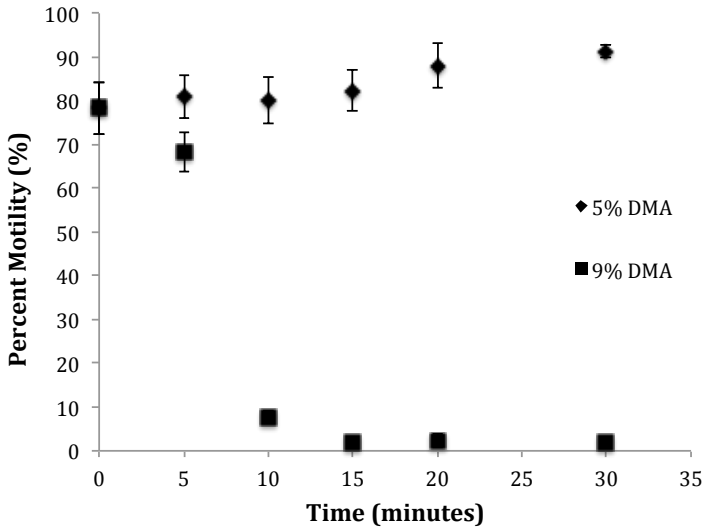

FIGURE 11: BENCH-TOP CRYOPROTECTANT LOADING. DMA solutions were prepared and introduced to cells in a test tube. At the time intervals indicated, an aliquot of sample solution was collected and activated with water for interrogation with CASA to produce motility measurements. Each aliquot was assessed three times to produce an average value at each time interval. Error bars represent standard deviation for samples tested for a given time interval.

On-chip Cryoprotectant Loading

For on-chip loading, the device was operated at 1 µL/min, a flowrate chosen to allow for downstream integration with current freezing practices (required freezing volumes) while allowing for appreciable cryoprotectant loading and dehydration. We do not see acceptable reproducibility from sample to sample and we see fairly large standard deviations within a sample.

TABLE 1: ON-CHIP TOXICITY ASSESMENT. Motility measurements for samples loaded with 9% DMA on-chip at 1 µL/min are shown. For each fish (sample), three different aliquots were collected and interrogated. Each sample motility measurement is an average of three different measurements taken on the same aliquot.

	Sample 1 4.16E+08 cells/mL	**Sample 2** 4.25E+08 cells/mL	**Sample 3** 4.25E+08 cells/mL
Initial Motility	78.3 ± 6.0	75.7 ± 8.3	71.7 ± 6.4
1	80.7 ± 4.9	69.7 ± 5.5	39.3 ± 13
2	94.7 ± 0.58	48.7 ± 1.2	52.3 ± 8.4
3	87.0 ± 3.6	45.6 ± 13	52.7 ± 13
Average	**87.4 ± 6.4**	**54.7 ± 13**	**48.1 ± 12**

4.3 Discussion & Conclusion

Though the results of the CPA loading on-chip experiments do not appear promising, these results are not conclusive. All samples tested on-chip were performed on the same chip over an extended period of time. Though the chip was flushed with HBSS to clear and clean the device at the end of each use, it is quite possible that issues with the device identified in the laboratory, such as bio-fouling (tissues, cells blocking parts of the channel) and consequentially trapped air bubbles, could have had an affect on the performance of the chip over time. An additional variable that could have influenced these results would be the DMA adsorption to PDMS. Another round of experiments in an identical device that does not adsorb organics should be performed in a short time period (ideally in the same day) to confirm or contradict the seeming irreproducibility of CPA loading on-chip.

Additional discussion of the chosen operating flowrate is also necessary. The flowrate chosen was selected based on the needs of current freezing protocols downstream, not for optimum cryoprotectant loading. At 1 µL/min with an average residence time of about 24 s, one can assume that mass transport across the membrane would be insufficient.

TABLE 2: ESTIMATED RESIDENCE TIMES IN CPA LOADING CHIP. From the dimensions of the channel geometry following the fluid junction, (50 µm x 200 µm x 12.5 cm) the volume of this CPA exposure portion of the channel is 1.25 µL. From this calculation, the residence time of a differential volume of a sample in the channel (and the exposure to DMA) can be estimated to by calculating the theoretical residence time of a cell travelling down the center streamline of the channel as a function of flowrate.

Inlet Flowrate [µL/min]	**Estimated Residence Time** [min:sec]	**Outlet Flowrate** [µL/min]
0.01	41:50	0.03
0.05	8:24	0.15
0.1	4:12	0.3
0.5	0:48	1.5
1	0:24	3
5	0:05	15
10	0:03	30

Identifying this issue, the toxicity effects of DMA loading on-chip at lower flowrates were investigated and we attempted to compare these to the bench-top process by correlating those flowrates to an estimated exposure time.

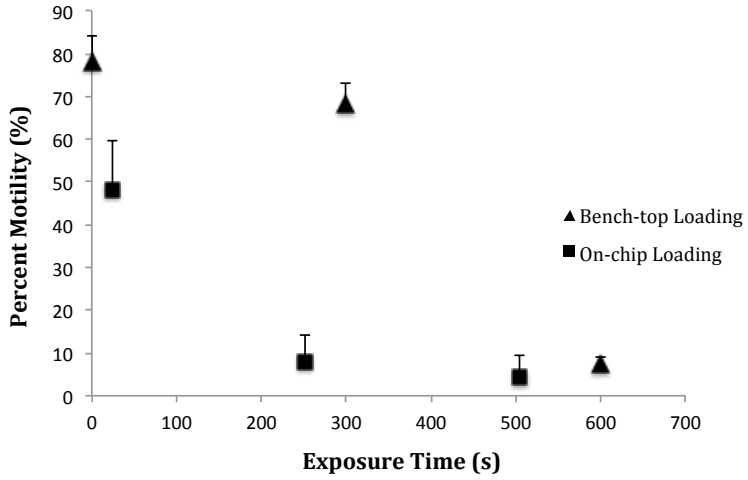

FIGURE 12: COMPARISON OF BENCH-TOP AND ON-CHIP LOADING TOXICITY. Toxicity of bench-top DMA loading is shown as a function of equilibrium time for a 9% DMA treatment. Toxicity of on-chip DMA loading of a 9% DMA treatment is shown as a function of estimated residence time for 1 µL/min, 0.1 µL/min, and 0.05 µL/min. For each motility measurements in both cases n > 5.

We again see seemingly discouraging results where the on-chip loading does not perform as well as the bench-top process, but these results are also not entirely conclusive. When operating at 0.1 µL/min, and 0.05 µL/min we achieve a more realistic exposure time on-chip, but at the expense of unrealistic outlet flowrates. As a consequence, cells exiting the channel lay at the outlet in the DMA solution until an appropriate volume for CASA interrogation has pooled at the outlet. In this case, all cells in the sample would experience a potential reduction in osmotic shock at the beginning of the treatment when they reach the fluid junction on chip, but a majority of the cells would be exposed to the CPA solution much longer than quoted based on residence time. This is not only a disadvantage for tempering toxicity effects, but also creates wider a distribution in cellular outcomes for a given sample. In the future, longer channel lengths should be utilized to allow operation at moderate flowrates while allowing for sufficient exposure time. Another potential solution to this problem would be to institute a mechanism for continuous freezing at the outlet of the chip. The downstream integration with continuous freezing protocols used in the food production industry would also enhance the high-throughput and automated nature of this proposed protocol.

In order to satisfy the recommendations of longer channel length, non-adsorbing channel materials, and integration with continuous freezing mechanisms, these microenvironments should move away from microfluidic devices ("microfluidic chips") to microfluidic tubing systems. The use of microfluidic tubing over a microfluidic chip could also reduce device failure due to pressure drops seen in the attempted operation of the cryoprotectant cocktail chip and reduce fabrication costs dramatically. In the design of a microfluidic tubing system, the cell sample should be injected and driven through a main line with pneumatic valving, and the CPA species should be introduced through a separate line joined to the main line through a minimum volume, 2-inlet junction. For cryoprotectant cocktail scenarios, multiple fluid junctions could be joined to the main line in a variety of configurations for optimum exposure time to each species in the cocktail. By modeling the fluid flow fields of potential configurations and using tubing over expensive microfabricated structures, rapid, inexpensive prototyping can produce the ideal high-throughput, low volume system for CPA loading at the microfluidic scale.

CHAPTER 5: FINAL CONCLUSIONS

The multidisciplinary work shown here is a strong first step in bringing microfluidic technology to the CPA loading process. Through mathematical modeling we are able to show the importance of balancing CPA exposure with membrane transport time through flowrate and the unique flow fields associated with viscous fluid interactions at a microscale. Experimentally, we were able to asses the feasibility of the introduction of this technology into laboratory practices and make recommendations on future efforts in bringing small volume, high-throughput methods to cryopreservation.

As more contributions are made to empirically deriving membrane transport parameters for cryoprotectants, modeling of cryoprotectant loading will become an effective tool for expediting the determination of new cryopreservation protocols and ultimately produce protocols with higher success rates due to the capacity for greater understanding of specific cell type and CPA species interactions at any volume scale. Additionally, cell type and CPA treatment specific microfluidic designs can be investigated and optimized *in silico* prior to device prototyping through the modeling strategies outlined here. Our translation of modeling efforts to experimental devices would greatly improve with the ability to use established membrane transport parameters to match a model to our intended experimental use. For instance, our koi sperm cell device design, which was based on our model for a human embryonic cell type, could have been greatly improved by a concrete knowledge of the inferred, yet neglected differences in membrane transport parameters for the two cell types.

For the future implementation of those systems in the laboratory, microfluidic tubing systems should be employed, but the ability to operate and assess the efficacy of such a system is currently dependent on upstream and downstream processes to the CPA loading process are still on a macro-scale. The assessment of the efficacy of these microfluidic strategies and their eventual introduction into laboratory process relies on the development of high-throughput, micro-scale formats for sample collection, freezing, and motility assessments.

Based on our knowledge of flow in a microchannel and the ability to fine-tune a cellular experience in a microchannel, positive cellular outcomes are possible in a small volume system with laminar flow. Even if claims for improvement through the proposed system proved an over-sell in the physical laboratory, the advantages of a system for high-throughput, reproducible methods for freezing and cataloging small samples would be important to society. For our partners in aquaculture, the ability to freeze the samples of individual, small-bodied fish in a reproducible, high-throughput manner would

expedite and improve their services for the aquaculture industry in the region. For our group, serving the interest of the biomedical research industry in cataloging small volumes of cell lines quickly and predictably would improve research efforts in biomedical industries. Lastly, as cellular therapies (tissue engineering strategies that involve introduction of human cellular constructs for tissue repair) gain momentum in biomedical research, comparable efforts in reliable, small volume technologies for the cryopreservation of cell types commonly extracted for use in cellular therapy should be pursued to ensure the technology can have relevance clinically.

In short, cryopreservation is an important tool in many fields and industries of interest to the public. Here we have provided a sturdy stepping-stone for future work in any of these fields for the development of small-volume, high-throughput and reproducible cryopreservation protocols.

REFERENCES

1. Babiak, I. et. al. (1997). *Cryopreservation of sperm of common carp, Cyprinus carpio L.* Aquculture Research **28**: 567-571.
2. Benson, J. D., et al. (2012). *Mathematical optimization of procedures for cryoprotectant equilibration using a toxicity cost function*. Cryobiology **64**(3): 144-151.
3. Blanco, J. M., et al. (2012). *Comparative cryopreservation of avian spermatozoa: effects of freezing and thawing rates on turkey and sandhill crane sperm cryosurvival*. Anim Reprod Sci **131**(1-2): 1-8.
4. Chen, H.-h., et al. (2008). *A microfluidic study of mouse dendritic cell membrane transport properties of water and cryoprotectants.* International Journal of Heat and Mass Transfer **51**(23-24): 5687-5694.
5. Chen, H.-h., et al. (2007). *Development of a microfluidic device for determination of cell osmotic behavior and membrane transport properties.* Cryobiology **55**(3): 200-209.
6. Clark, N. A. and J. E. Swain (2013). *Oocyte cryopreservation: searching for novel improvement strategies.* J Assist Reprod Genet **30**(7): 865-875.
7. Cuevas-Uribe, R. C. (2011). *A General Approach for Vitrification of Fish Sperm*. (Unpublished Doctoral Dissertation). Louisiana State University, Baton Rouge, Louisiana.
8. Cuevas-Uribe, R., et al. (2011). *Production of F(1) offspring with vitrified sperm from a live-bearing fish, the green swordtail Xiphophorus hellerii*. Zebrafish **8**(4): 167-179.
9. Cui, Z. F., et al. (2002). *Modeling of cryopreservation of engineered tissues with one-dimensional geometry*. Biotechnology Progress **18**(2): 354-361.
10. Dooley, K. and L. I. Zon (2000). *Zebrafish: a model system for the study of human disease*. Current Opinion in Genetics & Development 10(3): 252-256.
11. Eisenberg, D. P., et al. (2012). *Thermal expansion of the cryoprotectant cocktail DP6 combined with synthetic ice modulators in presence and absence of biological tissues*. Cryobiology **65**(2): 117-125.
12. Elder, E., et al. (2005). *Enhanced tissue strength in cryopreserved, collagen-based blood vessel constructs*. Transplant Proc **37**(10): 4625-4629.
13. Fahy, G. M., et al. (2004). *Improved vitrification solutions based on the predictability of vitrification solution toxicity*. Cryobiology **48**(1): 22-35.
14. Fleming, K. K., et al. (2007). *Numerical characterization of diffusion-based extraction in cell-laden flow through a microfluidic channel*. Journal of Biomechanical Engineering-Transactions of the Asme **129**(5): 703-711.
15. Fleming Glass, K. K., et al. (2008). *Optimization of a Microfluidic Device for Diffusion-Based Extraction of DMSO from a Cell Suspension*. Int J Heat Mass Transf **51**(23-24): 5749-5757.
16. Gerhard, G. S. (2003). *Comparative aspects of zebrafish (Danio rerio) as a model for aging research*. Experimental Gerontology 38(11-12): 1333-1341.
17. Gilmore, J.A., et. al. (1995). *Effect of cryopro- tectant solutes on water permeability of human spermatozoa*. Biology of reproduction **53**(5): 985–995.
18. Glenn, D. W., III (2002). *Effect of Extenders and Osmotic Pressure on Storage of Eggs of Ornamental Common Carp Cyprinus carpio at Ambient and Refrigerated Temperatures.* Journal of the World Aquaculture Society **33**(3): 254-267.
19. Glenn, D. W., III (1993). *Effect of Osmolality, Extender and Temperature on Gamete Storage of Koi Carp.* (Unpublished Masters Thesis). Louisiana State University, Baton Rouge, Louisiana.
20. Guha, A. and R. Devireddy (2010). *Polyvinylpyrrolidone (PVP) Mitigates the Damaging Effects of Intracellular Ice Formation in Adult Stem Cells.* Annals of Biomedical Engineering **38**(5): 1826-1835.
21. Guryev, V., M. J. Koudijs, et al. (2006). *Genetic variation in the zebrafish*. Genome Research 16(4): 491-497.

22. Hanna, J., Hubel, A., Lemke, E. (2012) *Diffusion-based extraction of DMSO from a cell suspension in a three stream, vertical microchannel*. Biotechnology and Bioengineering 109(9), 2316–2324
23. Heo, Y. S., et al. (2011). *Controlled loading of cryoprotectants (CPAs) to oocyte with linear and complex CPA profiles on a microfluidic platform*. Lab Chip **11**(20): 3530-3537.
24. Hu, E., et al. (2011). *High-throughput cryopreservation of spermatozoa of blue catfish (Ictalurus furcatus): Establishment of an approach for commercial-scale processing*. Cryobiology **62**(1): 74-82.
25. Iaffaldano, N., et al. (2012). T*he cryoprotectant used, its concentration, and the equilibration time are critical for the successful cryopreservation of rabbit sperm: dimethylacetamide versus dimethylsulfoxide.* Theriogenology **78**(6): 1381-1389.
26. Jing, R., C. Huang, et al. (2009). *Optimization of activation, collection, dilution, and storage methods for zebrafish sperm.* Aquaculture 290(1-2): 165-171.
27. Karlsson, J., Szurek, E.A., Higgins, A.Z., Lee, S.R. (2013) *Optimization of cryoprotectant loading into murine and human oocytes*. Cryobiology
28. Karlsson, J., Toner, M. (1996) *Long-term storage of tissues by cryopreservation: critical issues*. Biomaterials
29. Kedem, O. and A. Katchalsky (1961). A physical interpretation of the phenomenological coefficients of membrane permeability.
30. Kleinhans, F. W. (1998). *Membrane permeability modeling: Kedem-Katchalsky vs a two-parameter formalism.* Cryobiology **37**(4): 271-289.
31. Lane, M., et al. (1999). *Containerless vitrification of mammalian oocytes and embryos - Adapting a proven method for flash-cooling protein crystals to the cryopreservation of live cells.* Nature Biotechnology **17**(12): 1234-1236.
32. Lawrence, C. (2007). *The husbandry of zebrafish (Danio rerio): A review*. Aquaculture 269(1-4): 1-20.
33. Lawson, A., et al. (2011). *Cytotoxicity effects of cryoprotectants as single-component and cocktail vitrification solutions*. Cryobiology **62**(2): 115-122.
34. Lawson, A., et al. (2012). *Mathematical modeling of cryoprotectant addition and removal for the cryopreservation of engineered or natural tissues.* Cryobiology **64**(1): 1-11.
35. Li, L. Y. (2006). *Numerical simulation of mass transfer during the osmotic dehydration of biological tissues.* Computational Materials Science **35**(2): 75-83.
36. Mata, C., Longmire, E.K., McKenna, D.H., Glass, K.K., Hubel, A. (2008). *Experimental study of diffusion-based extraction from a cell suspension*. Microfluidics and Nanofluidics **5**(4): 529–540.
37. Ogier de Baulny, B. et. al. (1999). *Membrane Integrity, Mitochondrial Activity, ATP Content, and Motility of the European Catfish (Silurus glanis) Testicular Spermatozoa after Freezing with Different Cryoprotectants.* Cryobiology **39**: 177-184.
38. Park, D. S., et al. (2012). *Microfluidic mixing for sperm activation and motility analysis of pearl Danio zebrafish.* Theriogenology **78**(2): 334-344.
39. Park, S., et al. (2011). *On-chip characterization of cryoprotective agent mixtures using an EWOD-based digital microfluidic device*. Lab on a Chip **11**(13): 2212-2221.
40. Scherr, T., Pursley, S. et. al. (2014). *A numerical study on the loading of cryoprotectant cocktails-on-a-chip Part I: Interacting miscible viscous fluids.* Internation Journal of Heat & Mass Transfer. (Under Review)
41. Scherr, T., Pursley, S. et. al. (2014). *A numerical study on the loading of cryoprotectant cocktails-on-a-chip Part II: The cellular experience.* Internation Journal of Heat & Mass Transfer. (Under Review)
42. Scherr, T., Pursley, S. et al. (2013). *A numerical study on distributions during cryoprotectant loading caused by laminar flow in a microchannel.* Biomicrofluidics **7**(2).
43. Scherr, T., et al. (2012). *A planar microfluidic mixer based on logarithmic spirals*. Journal of Micromechanics and Microengineering **22**(5).

44. Segre, G. and A. Silberberg (1961). *Radial Partical Displacements in Poiseulle Flow of Suspensions.* Nature **189**(476): 209-&.
45. Song, Y. S., et al. (2009). *Microfluidics for cryopreservation.* Lab on a Chip **9**(13): 1874-1881.
46. Squires, T. M. and S. R. Quake (2005). *Microfluidics: Fluid physics at the nanoliter scale*. Reviews of Modern Physics **77**(3): 977-1026.
47. Thirumala, S., et al. (2005). *Transport phenomena during freezing of adipose tissue derived adult stem cells*. Biotechnology and Bioengineering **92**(3): 372-383.
48. Tiersch, T. R., et al. (2012). *Outlook for development of high-throughput cryopreservation for small-bodied biomedical model fishes.* Comparative Biochemistry and Physiology C-Toxicology & Pharmacology **155**(1): 49-54.
49. Tseng, H. Y., et al. (2011). *A Microfluidic Study of Megakaryocytes Membrane Transport Properties to Water and Dimethyl Sulfoxide at Suprazero and Subzero Temperatures*. Biopreserv Biobank **9**(4): 355-362.
50. Whitesides, G. M. (2006). *The origins and the future of microfluidics*. Nature **442**(7101): 368-373.
51. Xu, F., et al. (2010). *Multi-scale heat and mass transfer modelling of cell and tissue cryopreservation*. Philosophical Transactions of the Royal Society a-Mathematical Physical and Engineering Sciences **368**(1912): 561-583.
52. Yang, H., C. Carmichael, et al. (2007). *Development of a simplified and standardized protocol with potential for high-throughput for sperm cryopreservation in zebrafish Danio rerio*. Theriogenology 68(2): 128-136.
53. Yang, H., et al. (2010). *Evaluation of cryoprotectant and cooling rate for sperm cryopreservation in the euryhaline fish medaka Oryzias latipes*. Cryobiology **61**(2): 211-219.